

## Features of laser ablation of porous silicon in air

© E.I. Mavreshko<sup>1,2</sup>, A.A. Fronya<sup>1,2</sup>, G.V. Tikhonowski<sup>1</sup>, M.S. Grigoryeva<sup>1,2</sup>, I.N. Zavestovskaya<sup>3,1,2</sup>

<sup>1</sup> National Research Nuclear University „MEPh“,  
115409 Moscow, Russia

<sup>2</sup> Lebedev Physical Institute, Russian Academy of Sciences,  
119991 Moscow, Russia

<sup>3</sup> National Research Center „Kurchatov Institute“,  
123182 Moscow, Russia

E-mail: EGOR.MAV@yandex.ru

Received May 3, 2024

Revised August 23, 2024

Accepted October 30, 2024

The results of an experimental study of the ablation thresholds of monocrystalline and porous 77 and 96% silicon are presented. The morphology of the samples was studied after exposure to femtosecond laser radiation with a pulse energy of 1–10  $\mu\text{J}$ . The dependences of the size of the impact trace on the embedded laser energy are obtained, and the thresholds of laser ablation are determined. It has been found that at high porosity, the size of the ablation region grows faster with increasing energy than for monocrystalline silicon and silicon of lower porosity.

**Keywords:** laser ablation, porous silicon, ablation threshold.

DOI: 10.61011/SC.2024.10.59939.6565A

### 1. Introduction

Currently in medicine the discipline on creation biodegradable nanoscale platforms is actively developed, they inside the human organism during limited time period will operate as diagnostic and (or) therapeutic devices. For such applications search of natural and development of new biodegradable materials are performed. One of such materials can be semiconductor silicon [1,2]. In terms of biomedical applications the nanosilicon is unique material, in crystalline form it is biodegradable, biocompatible and non-toxic to living organism. Currently it is shown that nanosilicon can be synthesized in different nanoforms: nanoparticles, nanowires, nanostructured porous films etc. The porous silicon can be used as biodegradable nanoscale platform, for example, as container for delivering the therapeutic drug or diagnostic radiopharmaceutical agent [3–5].

Properties of the porous silicon depend on the method and technological parameters of its production [6]. Laser ablation allows obtaining chemically pure nanoforms, monitoring the concentration, size and degree of their crystallinity [7]. When selecting optimal conditions of the laser ablation the threshold of material laser ablation is important parameter. According to data of paper [8], the silicon ablation threshold also depends on porosity, the higher porosity is the lower ablation thresholds are.

On the other hand, there is need of laser synthesis of nanoparticle of other materials, which initially have porous structure. For example, for boron neutron capture therapy (BNCT) the boron nanoparticles are synthesized from targets formed by sintering of boron powder and its compounds [9,10]. Such targets can have porous structure [11], affecting the laser ablation. Due to this study of the laser ablation processes near threshold is important

for development of production technologies of biomedical nanoparticles of porous materials.

In the presented paper the laser ablation of silicon with different degree of porosity is studied. The dependence of exposure trace size on input laser energy are obtained, the laser ablation thresholds are determined.

### 2. Materials and study methods

The porous silicon films were obtained by electrochemical etching. During etching the electrolyte comprising fluoric acid and ethyl alcohol ( $\text{HF}:\text{C}_2\text{H}_5\text{OH}$  1:1) was used. As initial material the single-crystal wafer of silicon KDB of *p*-type with crystalline orientation of surface [100]  $460\ \mu\text{m}$  were used. Etching area was  $1.8\ \text{cm}^2$ . After etching the layer of porous silicon stayed on surface of silicon wafer. As a result samples of silicon films with porosity 77 and 96% were obtained.

Experiment of ablation of porous silicon layers was performed using femtosecond laser unit TETA 10 (Yb:KGW). The laser parameters were as follows: wavelength — 1032 nm, pulse width — 270 fs, pulse repetition frequency — 100 kHz. The laser radiation was focused on sample with lens, at that laser spot diameter on the target surface was  $\sim 50\ \mu\text{m}$ . The laser system was set such that laser beam provides trace in form of stripe. Scanning rate along stripe was 10 mm/s. For each sample the laser radiation exposure was performed at pulse energies of 1 to 10  $\mu\text{J}$  with step 1  $\mu\text{J}$ . The laser radiation interaction with silicon was performed in air. After exposure samples were studied by scanning probe microscopy in microscope TESCAN MAIA3.

Note that the paper investigates not craters formed by the point exposure of laser radiation on a sample (see, for

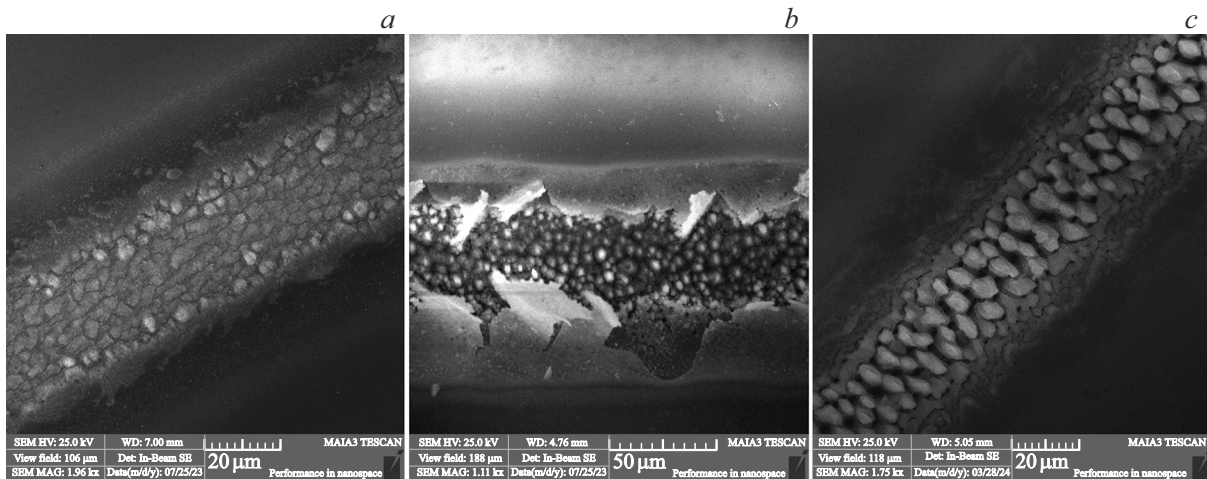


**Figure 1.** SEM-images of samples after exposure to laser radiation with energy  $9 \mu\text{J}$ : silicon with porosity 77% (a), silicon with porosity 96% (b), crystalline silicon (c).

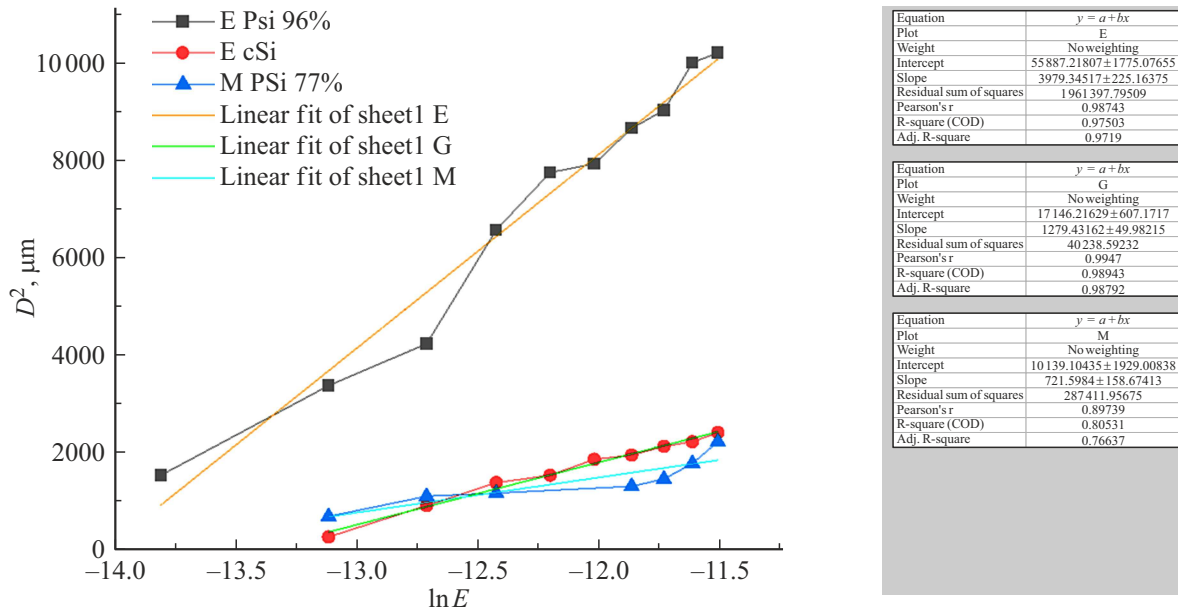


**Figure 2.** Square of width (diameter  $D$ ,  $\mu\text{m}$ ) of trace vs. laser radiation energy  $E$ , J.

example, [12,13]), but stripes formed by scanning with laser beam over the target surface, actually, in the mode that is used for the nanoparticles synthesis.

### 3. Experimental results and discussion

The laser beam has Gaussian distribution of energy, so in the stripe center the energy density is significantly higher than at edges. During such interaction in stripe we can see simultaneously several types of changes. As a result of morphology study of the ablation stripes two types of surface modification of samples can be detected. In the first case at low energies the trace is formed with smooth transition from center to edge, no breaks in substance

boundaries are observed. In second case with energy increasing of laser radiation the break boundaries are clearly detected along the scanning stripe, rather large structure of micron size formed in the stripe center are seen. For comparison, the results of experiments with single crystal silicon are presented, on its wafers samples of porous silicon were synthesized.

Figure 1 presents images of morphology of sample surface after study of radiation effect on the porous and crystalline silicon. To monitor visualization of exposure trace the photos were made using optical microscope. Note, that the exposure traces are clearly identified in both microscopes.

To determine the ablation thresholds we studied traces in form of stripes formed by the laser radiation at different energies of laser pulse. Using scanning electron microscopy

Threshold values of energy and energy density

Sample	$E_{th}$ , J	$W_{th}$ , J/cm <sup>2</sup>
Sample of porous silicon with porosity 96%	$7.8 \cdot 10^{-7}$	0.03
Sample of porous silicon with porosity 77%	$7.9 \cdot 10^{-7}$	0.13
Sample of crystalline silicon	$1.5 \cdot 10^{-6}$	0.15

(SEM) the width of stripes for each sample and values of laser radiation energy were determined.

As per data of papers [13,14], the ablation threshold can be determined from relationship

$$D^2 = 2\omega^2 \ln\left(\frac{E}{E_{th}}\right) = 2\omega^2 \ln E - 2\omega^2 \ln E_{th},$$

where  $D$  — ablation spot diameter ( $\mu\text{m}$ ),  $\omega$  — radius of Gaussian beam ( $\mu\text{m}$ ),  $E$  — pulse energy of laser radiation (J),  $E_{th}$  — threshold ablation energy (J).

Graph (Figure 2) presents square of width (diameter) of trace vs. laser radiation energy. The experimental data were approximated by a linear function, from which the threshold value of the energy of the ablation process was calculated. Deviations from the linear function in experimental curves are associated with possible sections of heterogeneous etching of wafer. Table shows the obtained values of ablation thresholds.

The obtained data show that ablation thresholds of porous samples are lower than for the crystalline silicon. Besides, graphs show that at high porosity the size of ablation area increases quicker with energy increasing than for the single crystal silicon and lower porosity. Note also that the ablation process of porous materials depends not only on the magnitude of porosity, but also on the size of the pores [8,12], which may be the reason for the significant differences between the two porous samples.

## 4. Conclusion

Paper presents the results of experimental measurement of the threshold value of laser ablation energy of porous and crystalline silicon. The laser ablation was performed in mode of sample surface scanning, most close to the procedure of nanoparticles synthesis. Study of size of exposure trace resulted in calculation of threshold values of laser ablation energy for samples with different degree of porosity and of single crystal silicon. The lowest threshold value was obtained for high-porosity silicon sample (96%) and was  $\sim 0.03 \text{ J/cm}^2$ .

## Funding

This study was supported financially by the Ministry of Science and Higher Education of the Russian Federation under agreement No. 075-15-2021-1347.

## Conflict of interest

The authors declare that they have no conflict of interest.

## References

- [1] R.K. Kankala, Y.H. Han, H.Y. Xia, S.B. Wang, A.Z. Chen. *J. Nanobiotechnology*, **20**, 126 (2022). <https://doi.org/10.1186/s12951-022-01315-x>
- [2] O.I. Ksenofontova, A.V. Vasina, V.V. Egorov, A.V. Bobyl, F.Yu. Soldatenkov, E.I. Terukov, V.P. Ulin, N.V. Ulin, O.I. Kiselev. *Techn. Phys.*, **59** (1), 66 (2014). DOI: 10.1134/S1063784214010083
- [3] L. Vaccari, D. Canton, N. Zaffaroni, R. Villa, M. Tormen, E. di Fabrizio. *Microelectron. Eng.*, **83** (4–9), 1598 (2006). <https://doi.org/10.1016/j.mec.2006.01.113>
- [4] I. Roy, S. Krishnan, A.V. Kabashin, I.N. Zavestovskaya, P.N. Prasad. *ACS Nano*, **16** (4), 5036 (2022). DOI: 10.1021/acsnano.1c10550
- [5] V.K. Tishchenko, V.M. Petrie, A.A. Mikhailovskaya, O.A. Smoryzanova, A.V. Kabashin, I.N. Zavestovskaya. *J. Phys.: Conf. Ser.*, **1439**, 012035 (2020). DOI: 10.1088/1742-6596/1439/1/012035
- [6] A.A. Ischenko, G.V. Fetisov, L.A. Aslanov. *Nanosilicon: properties, synthesis, applications, methods of analysis and control* (in Russian). (Fizmatlit, Moscow, 2011). ISBN: 978-5-9221-1369-4
- [7] T. Baati, A. Al-Kattan, M.A. Esteve, L. Njim, Yu. Ryabchikov, F. Chaspoul, M. Hammami, M. Sents, A.V. Kabashin, D. Braguer. *Sci. Rep.*, **6**, 25400 (2016). <https://doi.org/10.1038/srep25400>
- [8] A.Y. Kharin, M.S. Grigoryeva, I.N. Zavestovskaya, V.Y. Timoshenko. *Laser Phys. Lett.*, **18**, 076001 (2021). <https://doi.org/10.1088/1612-202X/ac0914>
- [9] S.A. Uspenskii, P.A. Khaptakhanova, A.A. Zaboronok, T.S. Kurkin, O.Y. Volkova, L.V. Mechetina, A.V. Tarantin, V.V. Kanygin, M. Akira, S.Y. Taskaev. *Dokl. Chem.*, **491**, 45 (2020). <https://doi.org/10.1134/S0012500820030027>
- [10] K.O. Aiyyzhy, E.V. Barmina, N.N. Melnik, O.V. Uvarov, G.A. Shafeev. *Bull. Lebedev Physics Institute*, **50**:suppl., S60 (2023). <https://doi.org/10.3103/S106833562313002X>
- [11] N.P. Bezhenar, A.A. Shulzhenko, S.A. Bozhko, G.S. Oleynik. *Phys. Technol. High Press.*, **17** (1), 21 (2007). (in Russian).
- [12] A.V. Skobelkina, F.V. Kashaev, A.V. Kolchin, D.V. Shuleiko, T.P. Kaminskaya, D.E. Presnov, L.V. Golovan, P.K. Kashkarov. *Techn. Phys. Lett.*, **46**, 687 (2020). <https://doi.org/10.1134/S1063785020070263>
- [13] Y. Wang, M. Zhang, Y. Huang, X. Cao, Y. Dong, J. Zhao, Y. Li, Y. Wang. *Optics Commun.*, **523**, 128608 (2022). <https://doi.org/10.1016/j.optcom.2022.128608>
- [14] J.M. Liu. *Optics Lett.*, **7**, 196 (1982). <http://dx.doi.org/10.1364/ol.7.000196>

Translated by I.Mazurov